A Time-Dependent Analysis for Vibrational and Chemical Nonequilibrium Nozzle Flows

JOHN D. ANDERSON JR.*
U. S. Naval Ordnance Lab., White Oak, Md.

An unsteady technique is presented for the numerical solution of quasi-one-dimensional, vibrational and chemical nonequilibrium nozzle flows including nonequilibrium conditions both upstream and downstream of the throat. This technique is a time-dependent analysis which entails the explicit finite-difference solution of the quasi-one-dimensional unsteady flow equations in steps of time, starting with assumed initial distributions throughout the nozzle. The steady-state solution is approached at large values of time. A virtue of the present time-dependent analysis is its simplicity, which prevails from its initial physical formulation to the successful receipt of numerical results. To exemplify the present analysis, results are given for several cases of vibrational and chemical nonequilibrium expansions through nozzles.

Nomenclature

A = cross-sectional area, also symbol for atomic species
A' = A/A^*
A^* = area of throat
a_0 = reservoir frozen speed of sound
a = speed of sound
a' = a/a_0
c_v = specific heat per unit mass of mixture
C_{v_i} = specific heat per mole of species i
E_i = internal energy per mole of species i, including the heat of formation
E_i' = E_i/E_0
E_0 = internal energy of the reservoir mixture
e_{vib} = vibrational internal energy per unit mass
e'_{vib} = e_{vib}/RT_0
h = Planck's constant
k = Boltzmann constant
$k_F{}^i$ = forward reaction rate constant
$k_R{}^i$ = reverse reaction rate constant; $k_F{}^i/k_R{}^i = K_e$
K_e = equilibrium constant
L = characteristic length taken equal to length of nozzle
p = pressure
q = general nonequilibrium variable in Eq. (5)
R = specific gas constant of the mixture
$\mathfrak{R}$ = universal gas constant
t = time
t' = $t/(L/a_0)$
T = temperature (translational)
T' = T/T_0
u = velocity
u' = u/a_0
V = $\ln u'$
$\dot{w}_i$ = rate of production of species i due to chemical reactions
x = distance along nozzle
x' = x/L
Z = $\ln \rho'$
α = mass fraction of atomic species in a dissociating gas
γ = c_p/c_v
Γ_i = $\ln \eta'_i$
η_i = mole-mass ratio of species i (moles of i per unit mass of mixture)
η'_i = η_i/η_0
η_0 = mole-mass ratio of the reservoir mixture
θ = $\ln(e'_{\text{vib}})$
ρ = density
ρ' = ρ/ρ_0
ν = characteristic vibrational frequency
τ = vibrational relaxation time
τ' = $\tau/(L/a_0)$
φ = $\ln T'$

Subscripts

i = denotes chemical species i
0 = reservoir conditions
A = denotes atomic species
A_2 = denotes diatomic species

Superscript

j = denotes collision partner in Eq. (14)

Received February 17, 1969; presented as Paper 69-668 at the AIAA 2nd Fluid and Plasma Dynamics Conference, San Francisco, June 16–18, 1969; revision received August 13, 1969. This research was supported jointly by the NOL Independent Research Funds and the Office of Naval Research.

* Chief, Hypersonics Group, Aerophysics Division. Member AIAA.

Introduction

BECAUSE of the practical importance of high-temperature flows through rocket nozzles and high-enthalpy aerodynamic testing facilities, intensive efforts have been made during the past decade to obtain relatively exact numerical solutions for the quasi-one-dimensional expansion of a high-temperature gas through a convergent-divergent nozzle when vibrational and/or chemical nonequilibrium conditions prevail within the gas both upstream and downstream of the throat. (See for example Refs. 1–13.) All of these nonequilibrium solutions involve steady-state analyses, and are by no means trivial; however, the evolution of such efforts has produced adequate and sophisticated techniques for the analysis of nonequilibrium nozzle flows. An authoritative discussion of these steady-flow techniques can be found in Ref. 1.

The purpose of the present paper is to present a useful, alternative approach for the numerical solution of quasi-one-dimensional nonequilibrium nozzle flows. This technique is a time-dependent analysis which entails the finite-difference solution of the quasi-one-dimensional unsteady equations of change in steps of time. For specified equilibrium reservoir conditions and a fixed nozzle shape, the physical gasdynamic properties are obtained in steps of time, starting with assumed distributions throughout the nozzle. The steady-state solution is approached at large values of time.

The present time-dependent analysis considers vibrational and chemical nonequilibrium conditions both upstream and downstream of the nozzle throat; the proper steady-state critical mass flow is automatically approached at large values of time. In addition, no oscillations and instabilities occur in regions of near equilibrium flow, no special procedures are required to start the solutions from equilibrium reservoir

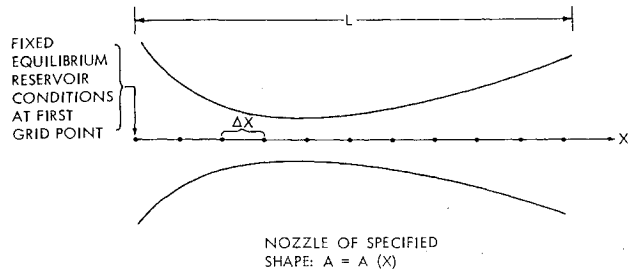

Fig. 1 Sketch of the coordinate system and grid points.

conditions, and very large spacings between grid points can be employed throughout the entire nozzle. (Accurate solutions have been obtained for convergent-divergent nozzles with area ratios of 10 using as few as 15 grid points beginning at the reservoir.) Also, the present method readily handles simultaneous rate processes involving very slow and very fast reactions.

The main virtue of the present time-dependent technique is its simplicity. The governing conservation equations are directly solved by a simple, explicit finite-difference scheme. The technique requires no additional mathematical methods to overcome special difficulties that can occur in the analysis of nonequilibrium flows. (See Ref. 1 for a detailed discussion of these difficulties.) Also, the present technique lends itself to particularly simple programing for a digital computer.

Analysis

The present analysis is based upon a Lax-Wendroff scheme as modified by Moretti and Abbett,[14] and further studied in Ref. 15. For specified equilibrium reservoir conditions and a fixed nozzle shape, initial values of the flowfield variables ρ, u, T, e_{vib} and chemical composition are assumed at equally spaced grid points along the x axis, as shown in Fig. 1. If all flowfield variables are known at time t, then at each grid point new values can be obtained at time $(t + \Delta t)$ from the first three terms of a Taylor's series expansion in time,

$$g(t + \Delta t) = g(t) + \left(\frac{\partial g}{\partial t}\right)_t \Delta t + (\partial^2 g/\partial t^2)_t[(\Delta t)^2/2] \quad (1)$$

where each term is evaluated at the local value of x, g signifies $\ln \rho$, $\ln u$, $\ln T$, $\ln (e_{vib})$, and $\ln \eta_i$, and Δt is a small increment in time chosen to satisfy certain stability criteria discussed in a subsequent section. Starting with the initially assumed gasdynamic variables at $t = 0$, the flowfield is subsequently obtained in steps of time from Eq. (1). At large values of time (after many time steps, usually on the order of 700 or more) the steady-state flowfield is obtained, where $\partial g/\partial t$ and $\partial^2 g/\partial t^2$ both approach zero.

The time derivatives $(\partial g/\partial t)_t$ and $(\partial^2 g/\partial t^2)_t$ which appear in Eq. (1) are obtained from the unsteady quasi-one-dimensional conservation equations[16] (the independent variables are x and t):

Continuity:

$$A\partial\rho/\partial t + \partial(\rho u A)/\partial x = 0 \quad (2)$$

Momentum:

$$\rho\partial u/\partial t + \rho u\partial u/\partial x = -\partial p/\partial x \quad (3)$$

Energy:

$$\rho\frac{\partial e}{\partial t} + \rho u\frac{\partial e}{\partial x} = -p\frac{\partial u}{\partial x} - pu\frac{\partial(\ln A)}{\partial x} \quad (4)$$

Rate:

$$\partial q/\partial t + u\partial q/\partial x = \dot{w}(\rho,T,q) \quad (5)$$

State:

$$p = \rho RT \quad (6)$$

where $A = A(x)$, q denotes a nonequilibrium quantity such as e_{vib} or chemical composition, and $\dot{w}$ is a function which depends on the type of rate process under consideration. Defining the following nondimensional variables, $\rho' = \rho/\rho_0$, $u' = u/a_0$, $T' = T/T_0$, $x' = x/L$, $t' = t/(L/a_0)$, $A' = A/A^*$, $Z = \ln\rho'$, $V = \ln u'$, $\phi = \ln T'$, where the subscript zero denotes reservoir conditions, L is the length of the nozzle, A^* is the nozzle throat area, and $a_0 = (\gamma_0 R_0 T_0)^{1/2}$ is the reservoir frozen speed of sound, and after replacing p in Eq. (3) with Eq. (6), Eqs. (2) and (3) become

$$\partial Z/\partial t' = -u'[\partial(\ln A')/\partial x' + \partial V/\partial x' + \partial Z/\partial x'] \quad (7)$$

$$\partial V/\partial t' = -(T'/\gamma_0 u')(\partial\phi/\partial x' + \partial Z/\partial x') - u'\partial V/\partial x' \quad (8)$$

[Note that Eq. (8) applies to a nonreacting gas, where R = const.; for a reacting gas, where R is variable, Eq. (8) is slightly modified.[17]]

In Eqs. (7) and (8), all x derivatives are calculated by central finite differences obtained from the known flowfield at time t;

$$\partial g/\partial x = [g(x + \Delta x) - g(x - \Delta x)]/2\Delta x$$

$$\partial^2 g/\partial x^2 = [g(x + \Delta x) - 2g(x) + g(x - \Delta x)]/(\Delta x)^2$$

Consequently, Eqs. (7) and (8) directly yield numbers for $(\partial g/\partial t)_t$ required in Eq. (1), where $g = Z$ and V; $(\partial^2 g/\partial t^2)_t$ can be obtained by differentiating the same equations with respect to time. However, this additional time differentiation introduces cross derivatives, $\partial^2 g/\partial x\partial t$, which can be obtained by differentiation of Eqs. (7) and (8) with respect to x. Complete details of these differentiations (as well as details of all other aspects of the present analysis) are presented in Ref. 17.

To complete the formulation of the problem, the nondimensional counterparts of Eqs. (4) and (5) must be obtained. These counterparts have a distinct form for each of the three cases treated in the present paper, namely the cases of a perfect gas, vibrational nonequilibrium, and chemical nonequilibrium.

Perfect Gas

By treating the case of a calorically and thermally perfect gas (constant γ), results have been obtained which illustrate the purely fluid dynamic behavior of the present time-dependent analysis. With $e = c_v T$ and $c_v = R/(\gamma - 1)$, the nondimensional form of Eq. (4) is

$$\frac{\partial\phi}{\partial t'} = -(\gamma - 1)u'\frac{\partial V}{\partial x'} - u'\frac{\partial\phi}{\partial x'} - (\gamma - 1)u'\frac{\partial \ln A'}{\partial x'} \quad (9)$$

Vibrational Nonequilibrium

The present time-dependent analysis has been applied to the vibrational nonequilibrium expansion of a pure diatomic gas. The vibrational mode is assumed to be in equilibrium within itself but not in equilibrium with the translational and rotational modes; i.e., a Boltzmann distribution is assumed to exist within the vibrational mode. Consequently, a vibrational temperature, not necessarily equal to the translational temperature, can be defined. With $e = \frac{5}{2}RT + e_{vib}$, Eq. (4) becomes

$$\frac{\partial T}{\partial t} = \frac{2}{5}\left[-T\frac{\partial u}{\partial x} - Tu\frac{\partial(\ln A)}{\partial x} - \frac{1}{R}\left(\frac{\partial e_{vib}}{\partial t} + u\frac{\partial e_{vib}}{\partial x}\right)\right] - u\frac{\partial T}{\partial x} \quad (10)$$

Defining $e'_{vib} = e_{vib}/RT_0$ and $\theta = \ln(e'_{vib})$, the nondimen-

sional form of Eq. (10) is

$$\frac{\partial \phi}{\partial t'} = -\frac{2}{5}\left(u'\frac{\partial V}{\partial x'} + u'\frac{\partial(\ln A')}{\partial x'} + \frac{e'_{\text{vib}}}{T'}\frac{\partial \theta}{\partial t'} + \frac{u'e'_{\text{vib}}}{T'}\frac{\partial \theta}{\partial x'}\right) - u'\frac{\partial \phi}{\partial x'} \quad (11)$$

In the rate equation, Eq. (5), $q = e_{\text{vib}}$ and $\dot{w}$ is assumed to be the relaxation equation for a harmonic oscillator. Therefore, Eq. (5) becomes

$$\frac{\partial e_{\text{vib}}}{\partial t} = \frac{1}{\tau}[(e_{\text{vib}})_{eq} - e_{\text{vib}}] - u\frac{\partial e_{\text{vib}}}{\partial x} \quad (12)$$

where τ is the vibrational relaxation time, $\tau = f(p,T)$, and $(e_{\text{vib}})_{eq}$ is the equilibrium vibrational energy evaluated at the local translational temperature of the gas, $(e_{\text{vib}})_{eq} = (h\nu/k) \times R/[\exp(h\nu/kT) - 1]$. Defining $\tau' = \tau/(L/a_0)$, the nondimensional form of Eq. (12) is

$$\frac{\partial \theta}{\partial t'} = \frac{1}{\tau'}\left[\frac{(e'_{\text{vib}})_{eq}}{e'_{\text{vib}}} - 1\right] - u'\frac{\partial \theta}{\partial x'} \quad (13)$$

Chemical Nonequilibrium

The present time-dependent analysis has also been applied to the case of a nonequilibrium dissociating symmetrical diatomic gas

$$A_2 + M_j \underset{k_{Rj}}{\overset{k_{Fj}}{\rightleftarrows}} 2A + M_j \quad (14)$$

where M_j is a collision partner (catalytic body); in the present application, $M_1 = A_2$ and $M_2 = A$. Also, chemical nonequilibrium is the only rate process considered; the vibrational energy is assumed to be in equilibrium with translation and rotation at the local gas temperature. Hence, for simplicity, no attempt is made to account for coupling between vibration and dissociation, even though such coupling effects may be important in some practical applications.[1] Letting subscript i denote a given chemical species, $e = \Sigma_i \eta_i E_i$, where η_i is the mole-mass ratio (moles of species i per unit mass of mixture), E_i is the molar internal energy of species i including its heat of formation, and $dE_i = C_{v_i}dT$. Also, the local frozen specific heat per unit mass of the mixture is $c_{v_f} = \Sigma_i \eta_i C'_{v_i}$, and the local value of the specific gas constant is $R = \mathfrak{R}\Sigma_i \eta_i$. In terms of the aforementioned quantities, Eq. (4) becomes

$$\frac{\partial T}{\partial t} = -\left(\frac{RT}{c_{v_f}}\right)\left(\frac{\partial u}{\partial x} + u\frac{\partial \ln A}{\partial x}\right) - u\frac{\partial T}{\partial x} - \frac{u}{c_{v_f}}\Sigma_i E_i \frac{\partial \eta_i}{\partial x} - \frac{1}{c_{v_f}}\Sigma_i E_i \frac{\partial \eta_i}{\partial t} \quad (15)$$

and Eq. (5) becomes

$$\frac{\partial \eta_i}{\partial t} = \dot{w}_i - u\frac{\partial \eta_i}{\partial x} \quad (16)$$

where $\dot{w}_i$ is the rate of production of species i by internal chemical reactions. Defining $\eta'_i = \eta_i/\eta_0$, $E'_i = E_i/E_0$, and $\Gamma_i = \ln\eta'_i$, where η_0 and E_0 are the reservoir values of the mixture mole-mass ratio and molar internal energy, respectively, nondimensional forms of Eqs. (15) and (16) are obtained as

$$\frac{\partial \phi}{\partial t'} = -\frac{R}{c_{v_f}}u'\left(\frac{\partial V}{\partial x'} + \frac{\partial \ln A}{\partial x'}\right) - u'\frac{\partial \phi}{\partial x'} - \left(\frac{E_0\eta_0}{T_0}\right)\left(\frac{1}{c_{v_f}T'}\right)\Sigma_i E'_i \dot{w}'_i \quad (17)$$

and

$$\partial\Gamma_i/\partial t' = \dot{w}'_i/\eta'_i - u'\partial\Gamma_i/\partial x' \quad (18)$$

where, for the atomic species

$$\dot{w}'_i = \dot{w}'_A = (L\rho_0\eta_0/a_0)\rho'[k_F^{(1)}(\eta'_{A_2})^2 + k_F^{(2)}(\eta'_{A_2})(\eta'_A)] - (L\rho_0^2\eta_0^2/a_0)(\rho')^2[(k_R^{(1)})(\eta'_A)^2(\eta'_{A_2}) + k_R^{(2)}(\eta'_A)^3] \quad (19)$$

Numerical Solution

Several comments are in order regarding numerical aspects of the present time-dependent method.

The initial conditions for ρ, u, and T are usually prescribed as linear variations or segments of linear variations with x. The initial values of ρ and T at the nozzle exit are chosen to be small, and u is chosen to be high, corresponding in an approximate, qualitative fashion to the supersonic solution. As a result, the transient solutions always converge to the steady, shock-free supersonic solution; at no time was a purely subsonic solution observed. Furthermore, in contrast to the original Lax-Wendroff scheme, the modified method employed in the present analysis does not allow the formation of distinct shock waves in the nozzle; if desired, shock waves could be explicitly inserted as discontinuities in the initial flowfield and handled in the same fashion as in the blunt-body solutions of Refs. 14 and 15. For convenience, the initial values for e_{vib} and η_i in the subsonic and throat regions are equilibrium values at the local assumed T and ρ, whereas at some arbitrary point downstream of the throat e_{vib} and η_i are usually set equal to constants for the remainder of the nozzle. Consequently, the initial distributions are at least qualitatively similar to the actual steady-state nonequilibrium distributions.

The initial conditions appear to have no meaningful effect upon either the stability or convergence of the technique; results have been obtained for identical nozzles and reservoir conditions but with widely different initial conditions, and in each case the same steady-state solution was obtained.

The time increment Δt appearing in Eq. (1) is chosen at the end of each time step to satisfy both the Courant-Friedrichs-Lewy stability criterion, where

$$\Delta t' \leq \Delta x'/(u' + a') \quad (20)$$

and a criterion geared to the speed of the nonequilibrium relaxation process

$$\Delta t' \leq B\Psi \quad (21)$$

where $\Psi = \tau'$ for vibrational nonequilibrium, $\Psi = \partial\dot{w}'_A/\partial\eta'_A$ for chemical nonequilibrium,[18] and B is a proportionality constant, found empirically to range from 0.8 to 0.2 for the present investigation. Both criteria must be satisfied simultaneously because two relaxation processes prevail in the time-dependent flow as it progresses towards the steady state; a fluid dynamic relaxation [Eq. (20)] involving the propagation and interaction of compression and expansion waves throughout the nozzle, and an internal physical-chemical relaxation [Eq. (21)] involving the finite rate processes of vibrational energy and chemical composition changes.

Because of the central differences employed in the present analysis, the flowfield variables at the first and last points in the grid (see Fig. 1) can not be directly obtained from Eq. (1). Instead, at the last point (nozzle exit) all the flow properties (in terms of Z, V, ϕ, etc.) are simply obtained from linear extrapolation from the two previous internal points. The first grid point (nozzle inlet) is considered to be effectively in the reservoir, i,e., A/A^* at this point is a large number, usually greater than ten. Hence, values of T and ρ at this point are assumed to be reservoir values and held fixed, invariant with time. The flow velocity (in terms of V) at this point is allowed to vary with time, and is found by linear extrapolation from the second and third internal points. At large values of time, the velocity at the inlet approaches its proper steady-state value (a very small but finite number)

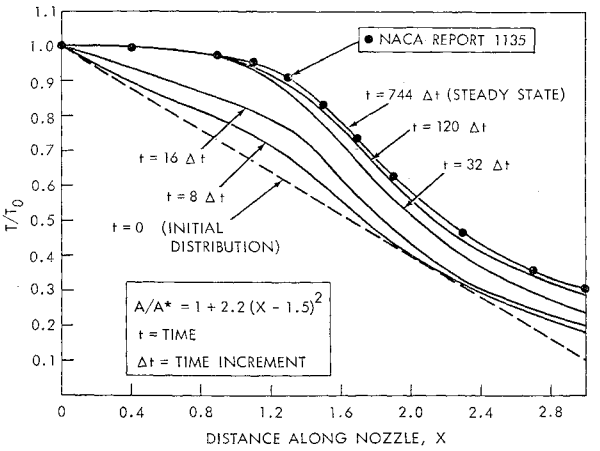

Fig. 2 Transient and final steady-state temperature distributions for a perfect gas obtained from the present time-dependent analysis; $\gamma = 1.4$.

compatible with the proper steady-state mass flow through the nozzle.

The computations are terminated when no change occurs in the fourth significant figure over an interval of 50 time steps; when this condition holds, the results are sufficiently close to the steady state.

As a final comment, the case of coupled slow and fast rate processes is readily treated [Eq. (21) must be satisfied for each rate]. This case has been tested by the present author in a separate, current study of non-Boltzmann population distributions established in a vibrational nonequilibrium expansion of a mixture of nonreacting gases, wherein the population of a given vibrational energy level is the result of several very slow and very fast, coupled rate processes. The results of this separate study will be published at a later date.

Results

Using the present time-dependent analysis, numerical results have been obtained on an IBM 7090 digital computer for the three cases of a perfect gas, vibrational nonequilibrium expansion of diatomic nitrogen, and the chemical nonequilibrium expansion of partially dissociated oxygen. As schematically shown in Fig. 1, the computations are made at equally spaced grid points along the nozzle. As few as 15 grid points are employed in a calculation; this is a convenient number and does not represent a required minimum for stability. Indeed, a virtue of the present time-dependent analysis is that large spacings between grid points can be employed throughout the nozzle, including the near equilibrium subsonic region near the reservoir.

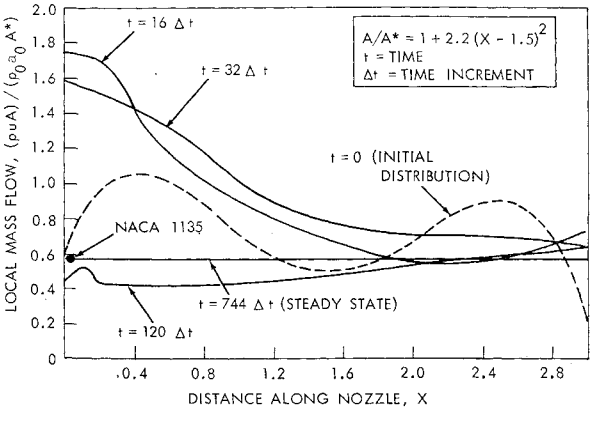

Fig. 3 Transient and final steady-state mass-flow distributions for a perfect gas obtained from the present time-dependent analysis; $\gamma = 1.4$.

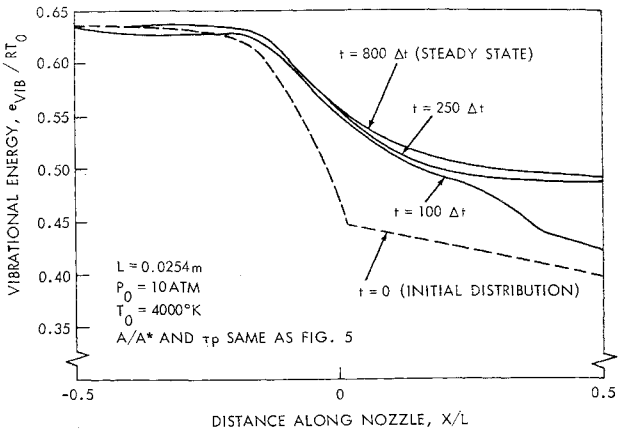

Fig. 4 Transient and final steady-state e_{vib} distributions for the nonequilibrium expansion of N_2 obtained from the present time-dependent analysis.

Perfect Gas

In order to investigate the purely fluid dynamic behavior of the present time-dependent analysis, results have been obtained for a perfect gas with $\gamma = 1.4$; some of these results are illustrated in Figs. 2 and 3. Starting with an initial linear distribution, the transient profiles of T' through the nozzle are shown at various time steps in Fig. 2. Two important points are noted from Fig. 2: 1) at early values of time, the profiles relax very rapidly to a steady-state distribution, and 2) the resulting steady-state distribution shows excellent agreement with known steady-state results obtained from Ref. 19. These results are complemented by the transient profiles of local mass flow, ρuA, through the nozzle, as shown in Fig. 3. The somewhat wavy initial distribution for ρuA is a consequence of the arbitrarily assumed initial distributions for ρ and u. Figure 3 markedly illustrates that the transient solution rapidly proceeds to the proper steady mass flow, ρuA = constant. This aspect of the present analysis is an important virtue when applied to nonequilibrium flows. Excellent agreement for the steady-state distributions of ρ and u is also obtained, as documented in detail in Ref. 17.

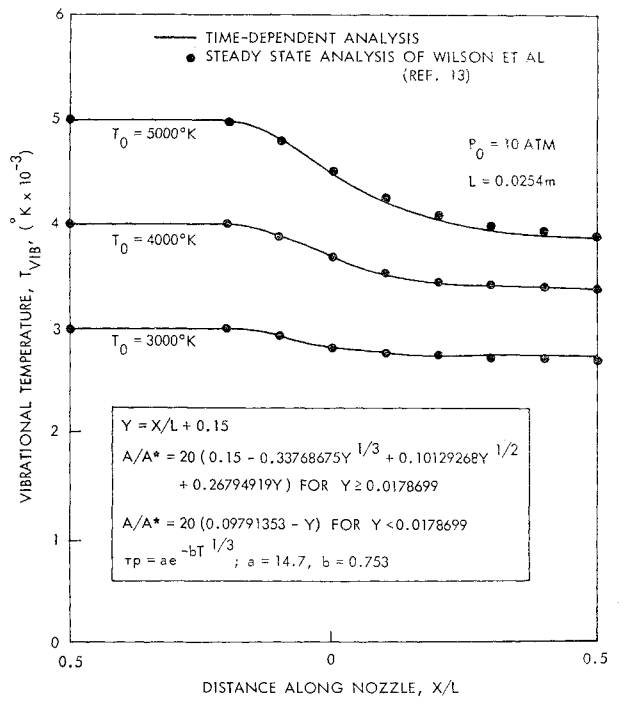

Fig. 5 Steady-state T_{vib} distributions for the nonequilibrium expansion of N_2; comparison of the present time-dependent analysis with the steady-flow analysis of Ref. 1

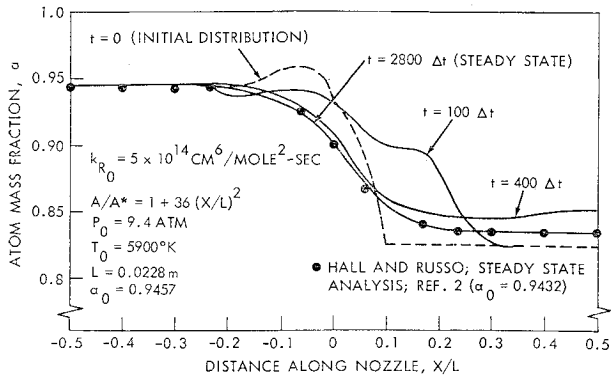

Fig. 6 Transient and final steady-state atom mass fraction distributions for the nonequilibrium expansion of dissociating oxygen obtained from the present time-dependent method; the steady-state distribution is compared with the steady-flow analysis of Ref. 2.

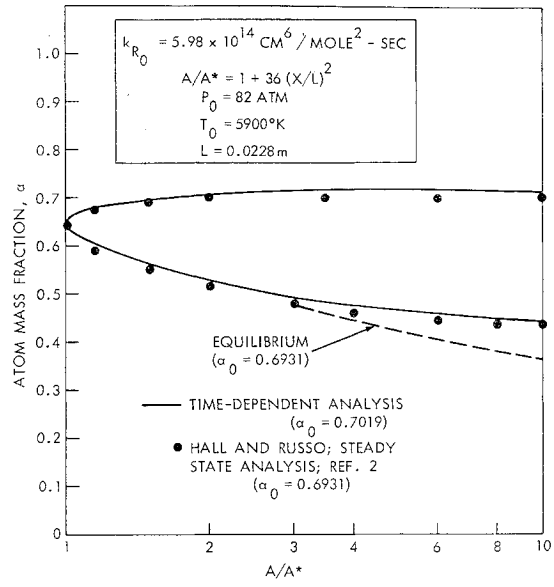

Fig. 7 Steady-state atom mass fraction distribution for the nonequilibrium expansion of dissociating oxygen; comparison of the present time-dependent analysis with the steady-flow analysis of Ref. 2.

Vibrational Nonequilibrium

Figures 4 and 5 illustrate results obtained with the present time-dependent analysis for the vibrational nonequilibrium expansion of N_2. For these results, the characteristic vibrational relaxation time was assumed to vary as $\tau p = a[\exp(-bT^{1/3})]$, following Ref. 8. The present results are obtained with $a = 14.7$ and $b = 0.915$, where p is in atm, T in °K, and τ in seconds. These values for a and b are fitted to the vibrational relaxation times used in Ref. 13, which reflect the shock-tube data of Blackman.[20] Of course, recent experiments have shown that vibrational relaxation times measured behind normal shock waves and subsequently used in Eq. (12) are not appropriate for expanding flows;[21] however, this does not detract from the present results, which are intended to illustrate the present time-dependent analysis and which are compared with earlier analyses using Blackman's shock-tube data.

To illustrate the time-dependent behavior of the vibrational nonequilibrium solution, Fig. 4 shows the transient e_{vib} profiles at various time steps; as in the previous case, a rapid approach to the steady-state distribution is observed. This steady-state distribution agrees with the results of a recent steady-flow analysis by Wilson et al.,[13] as shown in terms of T_{vib} in Fig. 5. Both the present time-dependent analysis and the steady-flow analysis of Ref. 13 include nonequilibrium effects upstream of the throat. The comparisons in Fig. 5 are made for several reservoir temperatures, and show very good agreement between the time-dependent and steady-flow approaches.

Chemical Nonequilibrium

Figures 6–8 illustrate results obtained with the present time-dependent analysis for the case of the chemical nonequilibrium expansion of partially dissociated oxygen

$$O_2 + M_j \underset{k_{Ri}}{\overset{k_{Fj}}{\rightleftarrows}} 2O + M_j$$

where $M_1 = O_2$ and $M_2 = O$. The reaction-rate constants and nozzle shape are taken identical to those of Hall and Russo,[1,2] where $k_R^{(1)} = k_{R_0}^{(1)}(T_0/T)$, $k_R^{(2)}/k_R^{(1)} = 35\ T/T_D$, $T_D = D/k$, D is the dissociation energy per molecule, and $k_F^j/k_R^j = K_e$. For the present results, the equilibrium constant, K_e, is obtained from Wray[22] as $K_e = (1.2 \times 10^3)\ T^{-1/2} \exp(-118{,}000/\mathcal{R}T)$, where K_e is in moles/cm³ and T in °K. Also, in the present results the vibrational energy is assumed to be in local thermodynamic equilibrium at the local gas temperature.

Figure 6 illustrates the transient profiles of atom mass fraction α at various time steps, where $\alpha = \rho_i/\rho = \eta_i \mathfrak{M}_i$. As in the previous cases, a continuous approach to the steady state is observed. However, in comparison with Figs. 2 and 4 from the previous cases, Fig. 6 shows that the steady state for the chemical nonequilibrium case is obtained after considerably more time steps. This behavior is due to the small values of Δt dictated by Eq. (21) for the present chemical nonequilibrium conditions; this contrasts to the previous results for the perfect gas and vibrational nonequilibrium cases, where the minimum Δt came from Eq. (20) and where the values of Δt were an order of magnitude larger than the present chemical nonequilibrium case. Also, in Fig. 6, the resulting steady-state distribution is compared to the results obtained from the steady-flow analysis by Hall and Russo;[2] very good agreement is obtained. (Note that a slight discrepancy occurs with the equilibrium reservoir mass fraction, α_0, which can be attributed to slight differences in K_e between the two sets of results.)

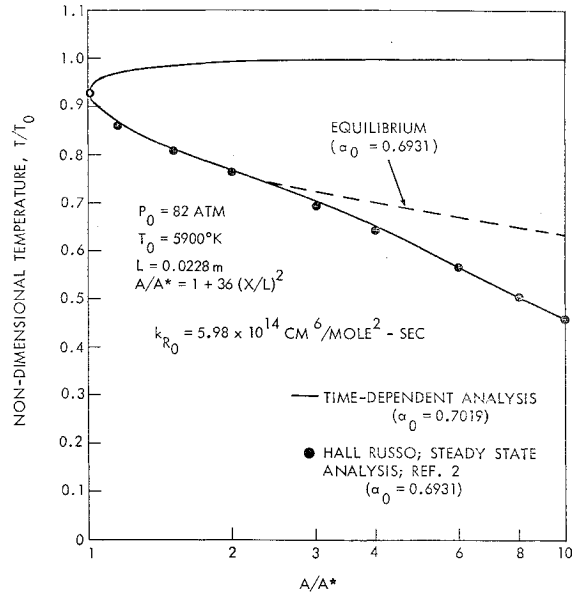

Fig. 8 Steady-state temperature distribution for the nonequilibrium expansion of dissociating oxygen; comparison of the present time-dependent analysis with the steady-flow analysis of Ref. 2.

Whereas the results shown in Fig. 6 are computed for $p_0 = 9.4$ atm, Figs. 7 and 8 show results obtained for $p_0 = 82$ atm, where equilibrium conditions are more closely approached, hence providing a more stringent test for the stability of a nonequilibrium flow analysis. Figures 7 and 8 show results obtained with the present time-dependent analysis for the steady-state α and T distributions, respectively (plotted versus nozzle area ratio). The upper branch of the curves applies to the subsonic section of the nozzle; the lower branch pertains to the supersonic section. These results are compared with the results of Hall and Russo, obtained from a steady-flow analysis. Very good agreement is obtained.

Conclusion

A useful, alternative solution for quasi-one-dimensional nonequilibrium nozzle flow is presented. The main virtue of this technique is its simplicity, which prevails from its initial physical formulation to the successful receipt of numerical results. Consequently, the time-dependent technique appears to warrant consideration for future applications in nonequilibrium nozzle flows.

References

[1] Hall, J. G. and Treanor, C. E., "Nonequilibrium Effects in Supersonic Nozzle Flows," CAL 163, March 1968, Cornell Aeronautical Laboratory, Buffalo, N.Y.; also AGARD-ograph 124.

[2] Hall, J. G. and Russo, A. L., "Studies of Chemical Nonequilibrium in Hypersonic Nozzle Flows," AFOSR TN 59-1090, Nov. 1959, Air Force Office of Scientific Research, Washington, D. C.

[3] Eschenroeder, A. Q., Boyer, D. W., and Hall, J. G., "Nonequilibrium Expansions of Air with Coupled Chemical Reactions," *The Physics of Fluids*, Vol. 5, No. 5, May 1962, pp. 615–624.

[4] Eschenroeder, A. Q., Boyer, D. W., and Hall, J. G., "Exact Solutions for Nonequilibrium Expansions of Air with Coupled Chemical Reactions," AFOSR 622, May 1961, Air Force Office of Scientific Research, Washington, D. C.

[5] Lordi, J. A. and Mates, R. E., "Nonequilibrium Expansions of High-Enthalpy Airflows," ARL 64-206, Nov. 1964, Aerospace Research Laboratories, Wright-Patterson AFB, Ohio.

[6] Mates, R. E. and Lordi, J. A., "Techniques for Solving Nonequilibrium Expanding Flow Problems," ARL 65-2, Jan. 1965, Aerospace Research Laboratories, Wright-Patterson AFB, Ohio.

[7] Stollery, J. L. and Park, C., "Computer Solutions to the Problem of Vibrational Relaxation in Hypersonic Nozzle Flows," Rept. 115, Jan. 1963, Imperial College of Science and Technology, London, England.

[8] Vincenti, W. G., "Calculations of the One-Dimensional Nonequilibrium Flow of Air Through a Hypersonic Nozzle—Interim Report," AEDC-TN-61-65, May 1961, Arnold Engineering Development Center, Tenn.

[9] Emanuel, G. and Vincenti, W. G., "Method for Calculation of the One-Dimensional Nonequilibrium Flow of a General Gas Mixture Through a Hypersonic Nozzle," AEDC-TDR-62-131, June 1962, Arnold Engineering Development Center, Tenn.

[10] Pearson, W. E., "Channel Flow of Gaseous Mixtures in Chemical and Thermodynamic Nonequilibrium," *The Physics of Fluids*, Vol. 10, No. 11, Nov. 1967, pp. 2305–2311.

[11] Moretti, G., "A New Technique for the Numerical Analysis of Nonequilibrium Flows," *AIAA Journal*, Vol. 3, No. 2, Feb. 1965, pp. 223–229.

[12] Lomax, H. and Bailey, H. E., "A Critical Analysis of Various Numerical Integration Methods for Computing the Flow of a Gas in Chemical Nonequilibrium," TN D-4109, Aug. 1967, NASA.

[13] Wilson, J. L., Schofield, D., and Lapworth, K. C., "A Computer Program for Non-Equilibrium Convergent-Divergent Nozzle Flow," National Physical Lab. Rept. 1250, Aeronautical Research Council No. A.R.C. 29246, Oct. 1967, London, England.

[14] Moretti, G. and Abbett, M., "A Time-Dependent Computational Method for Blunt Body Flows," *AIAA Journal*, Vol. 4, No. 12, Dec. 1966, pp. 2136–2141.

[15] Anderson, J. D., Jr., Albacete, L. M., and Winkelmann, A. E., "On Hypersonic Blunt Body Flow Fields Obtained with a Time-Dependent Technique," NOLTR 68-129, Aug. 1968, U. S. Naval Ordnance Lab., White Oak, Md.

[16] Liepmann, H. W. and Roshko, A., *Elements of Gasdynamics*, Wiley, New York, 1957.

[17] Anderson, J. D., Jr., "A Time-Dependent Analysis for Quasi-One-Dimensional Nozzle Flows with Vibrational and Chemical Nonequilibrium," NOLTR 69-52, May 1969, U. S. Naval Ordnance Lab., White Oak, Md.

[18] Vincenti, W. G. and Kruger, C. H., Jr., *Introduction to Physical Gas Dynamics*, Wiley, New York, 1965, p. 236.

[19] Ames Research Staff, "Equations, Tables, and Charts for Compressible Flow," Rept. 1135, 1953, NACA.

[20] Blackman, V. H., "Vibrational Relaxation in Oxygen and Nitrogen," *Journal of Fluid Mechanics*, Vol. 1, Pt. 1, May 1956, pp. 61–85.

[21] Hurle, I. R., Russo, A. L., and Hall, J. G., "Spectroscopic Studies of Vibrational Nonequilibrium in Supersonic Nozzle Flows," *Journal of Chemical Physics*, Vol. 40, No. 8, April 1964, pp. 2076–2089.

[22] Wray, K. L., "Chemical Kinetics of High Temperature Air," *Hypersonic Flow Research*, Academic Press, New York, 1962, pp. 181–204.